Pharm Res (2011) 28:597–609
DOI 10.1007/s11095-010-0311-7

RESEARCH PAPER

Galbanic Acid Isolated from *Ferula assafoetida* Exerts *In Vivo* Anti-tumor Activity in Association with Anti-angiogenesis and Anti-proliferation

Kwan-Hyun Kim • Hyo-Jung Lee • Soo-Jin Jeong • Hyo-Jeong Lee • Eun-Ok Lee • Hyun-Seok Kim • Yong Zhang • Shi-Yong Ryu • Min-Ho Lee • Junxuan Lü • Sung-Hoon Kim

Received: 17 May 2010 / Accepted: 25 October 2010 / Published online: 10 November 2010

ABSTRACT

Purpose To investigate whether galbanic acid (GBA) exerts anti-angiogenic and anti-cancer activities.

Methods Using human umbilical vein endothelial cell (HUVEC) model, we analyzed effects of GBA on cellular and molecular events related to angiogenesis. We tested its direct anti-proliferative action on mouse Lewis lung cancer (LLC) cells and established its *in vivo* anti-angiogenic and anti-tumor efficacy using LLC model.

Results GBA significantly decreased vascular endothelial growth factor (VEGF)-induced proliferation and inhibited VEGF-induced migration and tube formation of HUVECs. These effects were accompanied by decreased phosphorylation of p38-mitogen-activated protein kinase (MAPK), c-jun N-terminal kinase (JNK), and AKT, and decreased expression of VEGFR targets endothelial nitric oxide synthase (eNOS) and cyclin D1 in VEGF-treated HUVECs. GBA also decreased LLC proliferation with an apparent G2/M arrest, but did not induce apoptosis. *In vivo*, inclusion of GBA in Matrigel plugs reduced VEGF-induced angiogenesis in mice. Galbanic acid given by daily *i.p.* injection (1 mg/kg) inhibited LLC-induced angiogenesis in an intradermal inoculation model and inhibited the growth of *s.c.* inoculated LLC allograft in syngenic mice. Immunohistochemistry revealed decreased CD34 microvessel density index and Ki-67 proliferative index in GBA-treated tumors.

Conclusions GBA exerts anti-cancer activity in association with anti-angiogenic and anti-proliferative actions.

KEY WORDS angiogenesis · galbanic acid · HUVEC · Lewis lung cancer · mouse lung cancer · VEGF

K.-H. Kim • H.-J. Lee • S.-J. Jeong • H.-J. Lee • E.-O. Lee • S.-H. Kim (✉)
College of Oriental Medicine, Kyung Hee University
1 Hoegi-dong, Dongdaemun-gu
Seoul 130-701, Republic of Korea
e-mail: sungkim7@khu.ac.kr

K.-H. Kim • Y. Zhang • J. Lü (✉) • S.-H. Kim
The Hormel Institute, University of Minnesota
801 16th Avenue NE
Austin, Minnesota 55912, USA
e-mail: jlu@hi.umn.edu

H.-S. Kim
College of Medicine, Yonsei University
Seoul 120-752, Republic of Korea

S.-Y. Ryu
Korea Research Institute of Chemical Technology
Yuseong-gu
Daejeon 305-600, Republic of Korea

M.-H. Lee
College of Life Sciences, Kyung Hee University
Seoul 130-701, Republic of Korea

INTRODUCTION

Angiogenesis, the formation of new blood vessels from pre-existing vasculature, occurs under a variety of physiological and pathological conditions, including wound healing, embryonic development, chronic inflammation, and tumor progression and metastasis (1–4). Angiogenesis involves a series of coordinated events, including proliferation of endothelial cells (ECs), motility, cell realignment and vessel formation and production of a new basement membrane (1,2,4). Revascularization may be beneficial in the recovery from injuries such as ischemic stroke (5,6), but can also be detrimental to health in promoting tumor growth and metastasis, diabetic retinopathy and atherosclerosis (3,7). Accumulating evidence indicates that angiogenesis is especially critical for the growth and progression of solid tumors because growth of tumor mass beyond 2 to 3 mm^3

is often preceded by an increase in formation of new blood vessels essential for the delivery of nutrients and oxygen to and removal of metabolic wastes from the tumor microenvironment (1,3).

Therefore, anti-angiogenic therapy and angio-prevention represent promising approaches to control tumor growth and metastasis (8,9). As a proof of principle, human clinical trials in the last few years with anti-angiogenic modalities targeting vascular endothelial growth factor (VEGF) and its receptors, especially VEGFR-2 (KDR) using inactivating monoclonal antibodies or kinase inhibitor drugs, as single agents or in combination with chemotherapy, have shown survival benefit in cancer patients of an increasing number of advanced stage malignancies (10). Novel and safer agents are needed to complement existing modalities, especially in long-term prevention use. Interestingly, many anti-angiogenic agents currently under clinical trials are small molecule natural product compounds (9).

The genus *Ferula* belongs to the Umbelliferae family with approximately 130 species distributed throughout the Mediterranean and Central Asia, especially in the former Union of Soviet Socialist Republics (USSR) and neighboring countries. Oleogum resin obtained from the roots of *Ferula assafoetida* contains a number of bioactive compounds, including galbanic acid (GBA) (11) (Fig. 1a) and farnesiferol C (FC) (11,12). Galbanic acid is a sesquiterpene coumarin-containing compound, first isolated in 1973. Its structure was completely identified later by an analysis of 300 MHz ^{1}H NMR spectrum (13). However, the biological activities of GBA were not well studied except an inhibition of thrombocyte aggregation (14), which is a process closely associated with angiogenesis. Given that some coumarin compounds have been reported to possess anti-angiogenesis activity (15–17), especially in our recent work with the related coumarin compound FC (12), and that angiogenesis is critical for cancer growth and progression (1,2,4), we focused on anti-angiogenesis as one of the possible mechanisms for GBA to exert anti-cancer activity.

VEGF, secreted from a variety of tumors, is the most important angiogenic factor associated closely with induction and maintenance of the neovasculature in human tumors (10,18,19). Therefore, we assessed the inhibitory activity of GBA on a battery of VEGF-induced angiogenesis responses. Specifically, we purified GBA and evaluated its effects *in vitro* on VEGF-induced cell proliferation, migration and tube formation in human umbilical vein endothelial cells (HUVECs) and on VEGFR downstream proteins/kinases, including AKT, JNK and p38MAPK and cyclin D, endothelial nitric oxide synthase (eNOS). We also tested the direct impact of GBA on mouse Lewis lung carcinoma (LLC) cells in terms of cell proliferation and apoptosis. *In vivo,* we tested the efficacy of GBA on VEGF-induced angiogenesis in Matrigel plug model, neovessel formation induced by and the growth of highly angiogenesis-dependent LLC allograft inoculated in syngenic mice. We did immunohistochemistry with antibodies of Ki-67 for proliferative index and CD34 for microvessels density index. Our data suggest GBA (or its metabolites) exerts anti-cancer effect, primarily through anti-angiogenesis as well as anti-proliferation.

MATERIALS AND METHODS

Materials

Dulbecco's modified Eagle's medium (DMEM), Medium 199 (M199), phosphate-buffered saline (PBS), and fetal bovine serum (FBS) were purchased from WelGENE (Republic of Korea). Anti-biotic/mycotics were purchased from GIBCO (Grand Island, NY). XTT (2, 3-bis [2-methoxy-4-nitro-5-sulfophenyl]-2H-tetrazolium-5-carboxanilide) and PMS (N-methyldibenzo-pyrazine methyl sulfate) were from Sigma-Aldrich Chemical Co. (St. Louis, MO). The polyester membranes (12 μm pores) and 48-well chemotaxis chamber were purchased from Nuero Probe, Inc. (Cabin John, MD, USA). Protease inhibitor cocktail was from Boehringer Mannheim (Indianapolis, IN). DC protein assay kit II was from Bio-Rad (Hercules, CA). Antibodies for anti-phospho-AKT(Ser-473) (9271), phospho-eNOS(Ser-1177) (9571), phospho-p38 (Thr180/Tyr182) (9211), phospho-JNK (Thr183/Tyr185) (9251), anti- AKT(9272), anti-eNOS (9572), p38MAPK (9212) and JNK (9252) were from Cell Signaling Technology (Beverly, MA). Antibody for cyclin D1 (sc-753) was from Santa Cruz Biotechnology (Santa Cruz, CA). Anti-mouse ß-actin (A5316) was from Sigma-Aldrich. Goat anti-mouse IgG HRP conjugated secondary antibody and goat anti-rabbit IgG HRP conjugated secondary antibody were from Zymed (San Francisco, CA). 4× NuPAGE LDS sample buffer, 4–12% NuPAGE Bis-Tris gels and NuPAGE MES SDS running buffer were from Invitrogen (Carlsbad, CA). Hybond ECL transfer membrane and ECL western blotting detection kit were from Amersham Pharmacia (Arlington Heights, IL). X-ray films were from Agfa-Gevaert (CP-BU, N. V., Belgium). Antibodies for Ki-67 (M0879) was from Thermo Fisher Scientific (Fremont, CA). Antibodies for CD34 (ab8158) was from Abcam (Cambridge, UK). ABC kit (PK-6200), biotinylated anti-rabbit IgG secondary antibody (BA-1000) and DAB substrate Kit (SK-4100) were from Vector Lab., Inc. (Burlingame, CA, USA). Mayer's hematoxylin solution was purchased from Sigma-Aldrich (St. Louis, MO, USA) for counterstaining.

Isolation of Galbanic Acid

The gum resin of *F. assafoetida* was purchased from Hanil Herbal Shop, Seoul, Korea and was authenticated by

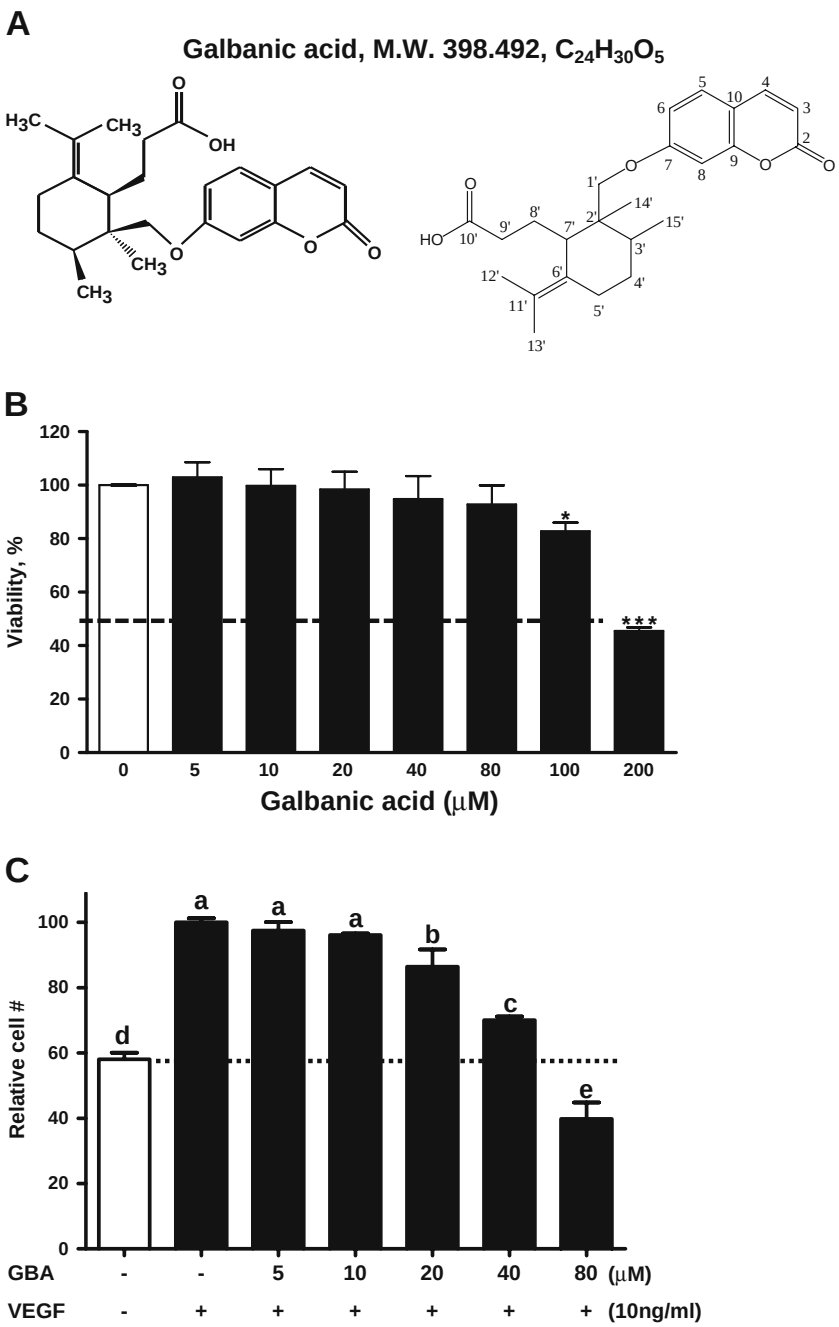

Fig. 1 **A** Two renditions of the chemical structure of galbanic acid (GBA) isolated from *Ferula assa-foetida* resin. The numbered structure (right) was provided for the NMR spectral references. **B** Effect of GBA on viability of non-proliferative HUVECs after 24 h exposure in serum-free medium. Viable cells were examined by XTT assay. Data were expressed as mean ± SE; $n=3$. $^{*}p<0.05$, $^{***}p<0.001$ compared with control. **C** Effect of GBA on VEGF-stimulated increase of viable cell number. Serum-starved HUVECs were exposed to DMSO or GBA in M199 containing 5% heat-inactivated FBS, heparin (5 unit/ml) and VEGF 10 ng/ml for 48 h, and the live cell number was assessed by XTT assay. Means bearing different letters are statistically different ($p<0.05$).

Dr. Namin Baek, professor of Department of Pharmaceutical Science, Kyung Hee University, Republic of Korea, and deposited at Cancer Preventive Material Development Research Center with voucher specimen number (2006-0808).

The gum resin of *F. assafoetida* (1.2 kg) was refluxed with methanol (MeOH) for 4 h. The solvent extract was collected and concentrated to dryness to give a crude extract (ca. 460 g), which was suspended in water and subjected to partition with hexane (56 g), methylene chloride (CH_2Cl_2, 290 g) and *n*-butanol (50 g), successively. Five grams of CH_2Cl_2 soluble fraction were purified by silica gel column chromatography and eluted with hexane and ethyl acetate (EtOAc) mixture in a gradient manner (R_f=0.3, hexane/EtOAc=3:1) to get 150 mg of compound, which was further purified by preparative TLC on silica gel and yielded crystalline (purity >99%) GBA. A direct comparison of physical and spectral properties (MS, $[\alpha]_D$, ^{1}H-NMR and ^{13}C-NMR) confirmed the chemical identity of GBA (13).

$$[\text{colorless needle}, [\alpha]_D - 20(\text{c}, 1.0 \text{ in } CHCl_3), C_{24}H_{30}O_5, \text{MW}398]$$

^{1}H NMR (300 MHz, $CDCl_3$) δ 7.60 (1H, d, J=9.5 Hz, H-4), 7.30 (1H, d, J=8.5 Hz, H-5), 6.78 (1H, dd, J=8.5, 2.4 Hz, H-6), 6.71 (1H, d, J=2.4 Hz, H-8), 6.20 (1H, d, J=

9.5Hz, H-3), 3.83 (1H, d, J=8.4 Hz, H-1′a), 3.66 (1H, d, J=8.4 Hz, H-1′b), 2.92 (1H, dd, J=11.1, 4.9 Hz, H-7′), 2.45 (1H, m, H-5′a), 2.17 (2H, m, H-9′), 1.82 (4H, m, H-5′b, 3′, 8′), 1.57 (3H, s, H-13′), 1.55 (1H, m, H-4′a), 1.40 (3H, s, H-12′), 1.15 (1H, m, H-4′b), 1.10 (3H, s, H-14′), 0.87 (3H, d, J=6.9 Hz, H-15′).

^{13}C NMR (125 MHz, $CDCl_3$) δ 180.1 (C-10′), 162.7 (C-2), 161.4 (C-7), 155.8 (C-9), 143.5 (C-4), 129.4 (C-6′), 128.5 (C-5), 126.1 (C-11′), 113.1 (C-6), 112.6 (C-3), 112.2 (C-10), 101.0 (C-8), 71.5 (C-1′), 42.5 (C-7′), 40.6 (C-2′), 34.7 (C-3′), 32.0 (C-9′), 31.8 (C-4′), 24.3 (C-5′), 22.4 (C-14′), 21.9(C-8′), 20.1 (C-12′, 13′), 15.9 (C-15′).

Isolation and Culture of Human Umbilical Vein Endothelial Cells

Human umbilical vein endothelial cells (HUVECs) were prepared for primary culture from human umbilical cord veins by method of Jaffe *et al.* (20) as we have reported previously (21). In brief, human umbilical cord veins were cannulated and flushed with cold phosphate-buffered saline (PBS) 0.2% glucose to remove blood and then filtered with 0.1% collagenase type I in PBS for 10 min at 37°C. After pelleting and resuspending twice, cells were plated in a 75 cm^2 tissue culture flask coated with 0.1% gelatin and allowed to adhere for 4 h. The culture flask was washed with Hanks' balanced salt solution (HBSS) to remove any nonadherent cells. The remaining adherent endothelial cells were maintained in M199 plus 20% heat-inactivated fetal bovine serum (FBS), 3 ng/ml bFGF, 5 units/ml heparin, 100 units/ml antibiotic-antimycotic solution (complete M199) in 0.1% gelatin-coated flasks and incubated at 37°C in a humidified atmosphere containing 5% CO_2. Once confluent, the cells were detached by trypsin-EDTA solution and used in experiments from the third to the sixth passages.

Cytotoxicity Assay Under Non-proliferating Condition

The cytotoxicity of GBA was determined by an XTT colorimetric method (22) under conditions of non-proliferation. HUVECs were seeded onto 0.1% gelatin-coated 96-well microplates at a density of 1×10^4 cells per well in 100 µl of complete M199 medium. After incubation at 37°C in a humidified incubator for 24 h, cells were treated with various concentrations (up to 200 µM) of GBA in serum-free M199 basal medium. After incubation for 24 h, XTT working solution was added to each well. Cells were incubated at 37°C for 2 h, and the optical density was measured using microplate reader (Molecular Devices Co.) at 450 nm. Cell viability was calculated as a percentage of viable cells in GBA-treated group *versus* vehicle-treated control by following equation: Cell viability (%) = [OD(GBA) − −OD (Blank)/OD(DMSO) − −OD(Blank)] ×100

VEGF-Stimulated Proliferation Assay

Mitogen-activated HUVEC proliferation assay was examined using XTT as described previously (12,21). HUVECs were seeded onto 0.1% gelatin-coated 96-well microplates at a density of 5×10^3 cells per well in 100 µl of complete M199 medium and incubated in a humidified incubator for 24 h. The cells were starved for 6 h in M199 containing 5% heat-inactivated FBS and then treated with various concentrations (up to 80 µM) of GBA in M199 containing 5% heat-inactivated FBS, 10 ng/ml VEGF and 5 units/ml heparin. After 48 h incubation, XTT working solution was added, and then the optical density was measured using microplate reader (Molecular Devices Co.) at 450 nm.

Migration/Invasion Assay

HUVEC migration/invasion assay was performed using a modified 48-well microchemotaxis chamber (Nuero Probe, Inc., Cabin John, MD) with polyester membrane, 25× 80 mm, and 12 µm pore size. The membrane was coated with 0.1% gelatin for 30 min and dried. The lower chamber was loaded with M199 containing HT1080 cell-conditioned medium (50:50, 0.1% BSA). The coated membrane and upper chamber were laid over the lower chamber. The upper chamber wells were then loaded HUVECs (4×10^4) in M199 containing 0.1% BSA, 5% heat-inactivated FBS, without or with 10 ng/ml VEGF and 5 units/ml heparin with increasing GBA (up to 40 µM). After incubation for 4 h at 37°C in 5% CO_2, membrane was fixed with Diff-Quick fixative and stained with Diff-Quick Sol. I and II, randomly chosen fields were photographed under an Axiovert S 100 light microscope (Carl Zeiss, Inc., USA) at × 100 magnification, and migrated cells were counted.

Tube Formation Assay

Assay for HUVEC *in vitro* differentiation into capillary-like tubes was performed on Matrigel by method of Grant *et al.* (23) as we have reported previously (21,24). Briefly, 24-well plates were coated with growth factor-reduced Matrigel (Becton Dickinson Labware, Bedford, MA) by incubating at 37°C for 30 min. HUVECs (4×10^4) were seeded per well with or without GBA in M199 containing 1% heat-inactivated FBS, 10 ng/ml VEGF and 5 units/ml heparin. After 6 h incubation, cells were fixed with 4% paraformaldehyde, randomly chosen fields were photographed under an Axiovert S 100 light microscope (Carl Zeiss, Inc., USA)

at ×100 magnification, and the number of tubes formed was counted.

Lewis Lung Carcinoma (LLC) Cells

LLC cells were obtained from Dr. I. Saiki (Toyama Medical and Pharmaceutical University, Toyama, Japan). Cells were cultured in DMEM supplemented with 10% heat-inactivated FBS, 25 mM HEPES buffer, 100 units/ml antibiotic/mycotics and 2 g/L sodium bicarbonate at 37°C in a humidified atmosphere containing 5% CO_2 as we reported previously (21).

The direct impact of GBA on LLC cell cycle and survival was evaluated in the presence of complete medium. LLC cells were plated into 6-well plate at a density of 10^5 cell/ml and treated with various concentrations of GBA. After 24 or 48 h incubation, total number of cells was counted using hemocytometer. Cells were analyzed for cell cycle distribution and by Western blot for cleavage of PARP and caspase-3 as biomarkers of apoptosis.

Western Blotting

HUVECs (4×10^5) treated with GBA were collected and washed with cold PBS. Cell pellets were lysed and used for WB as reported previously (21). The dilution rate of primary antibodies of anti-phospho-AKT(1:1000 dilution), phospho-eNOS(1:500 dilution), cyclin D1 (1:1000 dilution), phospho-p38MAPK (1:1000 dilution), phospho-JNK (1:1000 dilution), anti-AKT(1:1000 dilution), anti-eNOS (1:1000 dilution), p38MAPK (1:1000 dilution), JNK (1:1000 dilution). To normalize loading, used membranes were soaked in stripping buffer (62.5 mM Tris-HCl, pH 6.8, 150 mM NaCl, 2% SDS, 100 mM ß-mercaptoethanol) at 65°C for 30 min and hybridized with mouse anti-human ß-actin (1:2000 dilution).

Matrigel Plug Assay

Female C57BL/6 mice were purchased from Daehan Biolink Co. (Chungbuk, Korea) and given food and water *ad libitum*. Mice were housed in a room maintained at 25±1°C with 55% relative humidity. The Matrigel plug assay was performed as described by Passaniti *et al.* (25). Briefly, C57BL/6 mice (6 weeks old) were given s.c. injection of 0.5 ml of growth factor reduced Matrigel (Becton Dickinson Labware, Bedford, MA) containing GBA (20 µg/ml or 10 µg/plug), VEGF (10 ng/ml or 5 ng/plug) and heparin (10 U/ml). After 7 days, mice were sacrificed, and the Matrigel plug was removed. To quantify the formation of new blood vessel, the amount of hemoglobin (Hb) was measured using the Sigma BCS Hemoglobin assay kit (MF2101-01). The concentration of Hb was calculated from standard curve made from the known amount of Hb provided according to the manufacturer's protocol.

Tumor Cell-Induced Angiogenesis

LLC cells in subconfluent condition were harvested and resuspended in sterile PBS. C57BL/6 mice were inoculated intradermally with LLC cells of 5×10^5/cells in 50 µl PBS on the back of mice. Galbanic acid was administered by *i.p.* injections of 0.1 mg/kg and 1 mg/kg in PBS per day starting from 3 days after tumor cell inoculation. These dosages were chosen based on an assumption of achieving circulating levels of GBA modeled in the *in vitro* models to exert anti-angiogenic action. Ten days after the tumor inoculation, the mice were sacrificed, and the tumor-inoculated skin was separated from the underlying tissues. Angiogenesis was quantified by counting only the vessels directly supplying the tumor under a dissecting microscope.

Tumor Growth in LLC Allograft Bearing Mice

LLC cells in subconfluent condition were harvested and resuspended in sterile PBS. LLC cells (5×10^5 in 200 µl PBS) were subcutaneously injected into the right flank of C57BL/6 mice. Twelve days after tumor inoculation, mice were given once daily *i.p.* injection of GBA (0.1 mg/kg or 1 mg/kg in PBS). Tumor volumes were measured every other day with a caliper and calculated according to the formula $\left[(\text{length}\times\text{width}^2)/2\right]$, where length represents the largest tumor diameter, and width represents the smallest tumor diameter (26,27). All mice were sacrificed 18 days after tumor inoculation, and the tumors were excised and weighed.

Immunohistochemistry

Tumor specimens were immediately removed from sacrificed mice and prepared for histological examination. Tumors were fixed in 10% neutral buffered formalin overnight, embedded in paraffin, and sectioned to 4 µm thickness. The tumor sections were immobilized and deparaffinized by immersing in xylene, rehydrated in a graded series of ethanol and washed with distilled water (D.W.). For antigen retrieval, the tumor sections were boiled in 10 mM sodium citrate buffer (pH 6.0) for 15 min and cooled at room temperature. After washing with PBS, they were treated with 3% H_2O_2-methanol for 10 min at room temperature to quench endogenous peroxidase activity and blocked in 6% horse serum for 30 min in humidity chamber at room temperature. The sections were stained with Ki-67 (1:200 dilution in PBS with 1% BSA) and CD34 (1:50 dilution in PBS with 1% BSA) overnight at 4°C. After washing off primary antibodies, they developed color using ABC and DAB kits according to the manufacturer's protocols and

were counterstained with Mayer's hematoxylin solution. All stained sections were photographed under an Axiovert S 100 light microscope (Carl Zeiss, Inc., USA).

Statistical Analysis

The results were expressed as mean ± SE. Statistical significance was compared between GBA-treated group and control by the Student's *t*–test. Results with $p<0.05$ were considered significantly different from control.

RESULTS

Defining Cytotoxic Concentration Ranges of GBA for HUVECs and LLCs

We first determined the viability of HUVECs treated with GBA in serum-free medium without added angiogenic growth factors (i.e., non-proliferative) by XTT assay. GBA exposure for 24 h decreased the mitochondrial metabolic viability of HUVECs at 100 μM (Fig. 1b). GBA at 200 μM caused a significant decrease of this parameter by 55%.

In LLCs, exposure to GBA for as high as 200 μM in complete medium for 24 or 48 h did not cause any increase of biomarkers of caspase-mediated apoptosis, i.e., no cleavage of PARP or caspase-3 (Fig. 2a). Cell cycle analyses by flowcytometry did not detect an evident change of apoptotic sub G1 population (Fig. 2c, marked as M1 ranges). These results suggested that GBA might be more cytocidal to endothelial (HUVEC) than to cancer (LLC) cells.

Effect of GBA on VEGF-Inducible Proliferation of HUVECs and on LLC Cell Proliferation

To determine whether GBA affects mitogen-activated vascular endothelial cell proliferation crucial for angio-

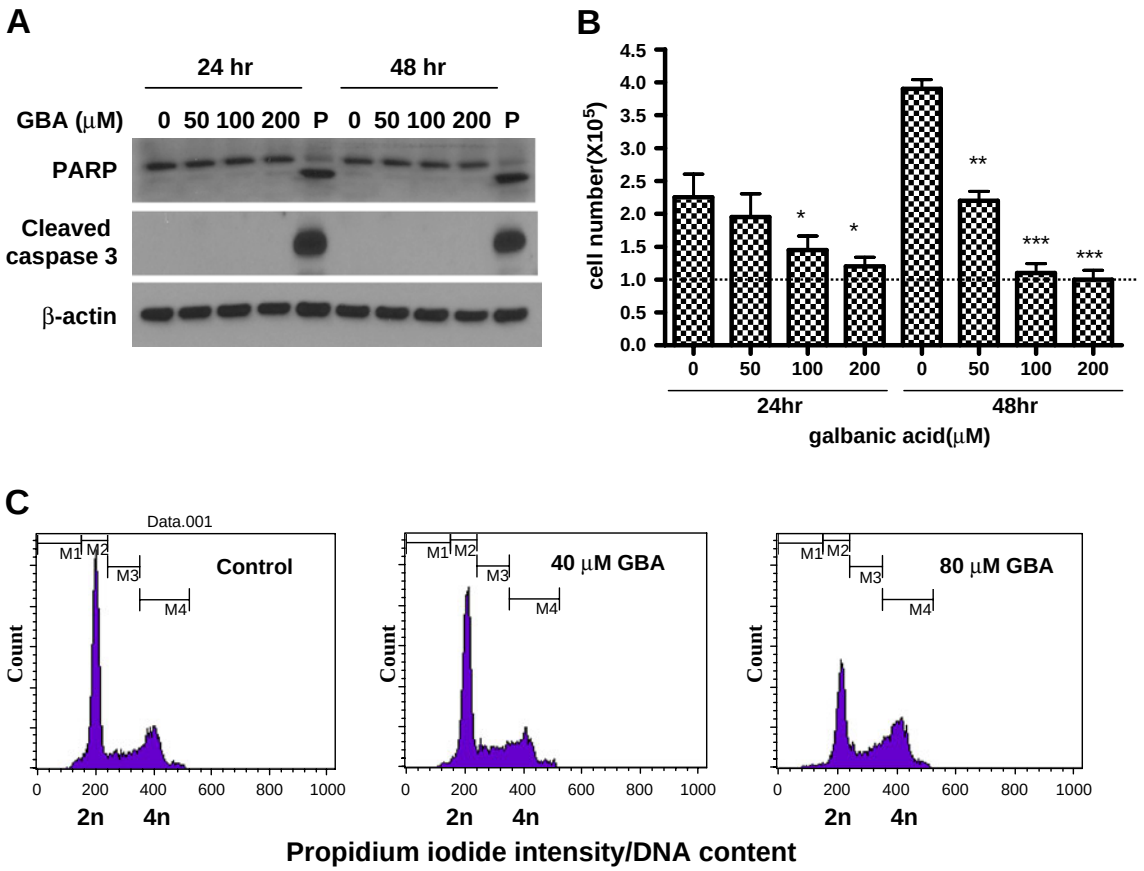

Fig. 2 Anti-proliferative effect and (lack of) apoptotic effect of GBA on LLC cells. **A** LLC cells were treated with various concentrations of GBA for 24 or 48 h. Cell lysates were analyzed by Western blotting for cleavage status of PARP, caspase-3. Lysate from tanshinone IIA-treated KBM-5 cells was used as a positive control (P) for apoptotic caspase activation. **B** LLC cells were plated to 6-well plate and treated with various concentrations of GBA. After 24 or 48 h incubation, total number of cells were counted using hemocytometer. The dash line marked the initial number of cells prior to GBA exposure. Graphs represent mean ± SD from three independent experiments. *$p<0.05$, **, $p<0.01$, ***$p<0.001$ compared with respective untreated control at each time point. **C** Representative patterns of flowcytometric distribution of LLC cells treated with GBA for 48 h. M1 marks sub-G1 apoptotic cells.

genic response, we examined the proliferation of HUVECs stimulated by VEGF (10 ng/ml) in the presence of various non-cytotoxic concentrations of GBA for 48 h. Galbanic acid significantly suppressed VEGF-induced proliferation (the difference between VEGF-stimulated control and basal control) by 33% and 71% at the concentrations of 20 and 40 μM, respectively (Fig. 1c). The estimated IC_{50} to inhibit VEGF-induced proliferation is ~30 μM. At 80 μM, the cell number was even lower than the un-stimulated basal control, indicating a cytocidal activity.

In LLC cells, GBA decreased cell growth in a concentration-dependent manner with IC50 ~80 μM for 24 h exposure and ~50 μM for 48 h exposure (Fig. 2b, dash line marked the initial LLC cell number prior to GBA treatment). The anti-proliferative effect in LLC cells was associated with a G2/M arrest (Fig. 2c). These data suggested a direct anti-proliferative action of

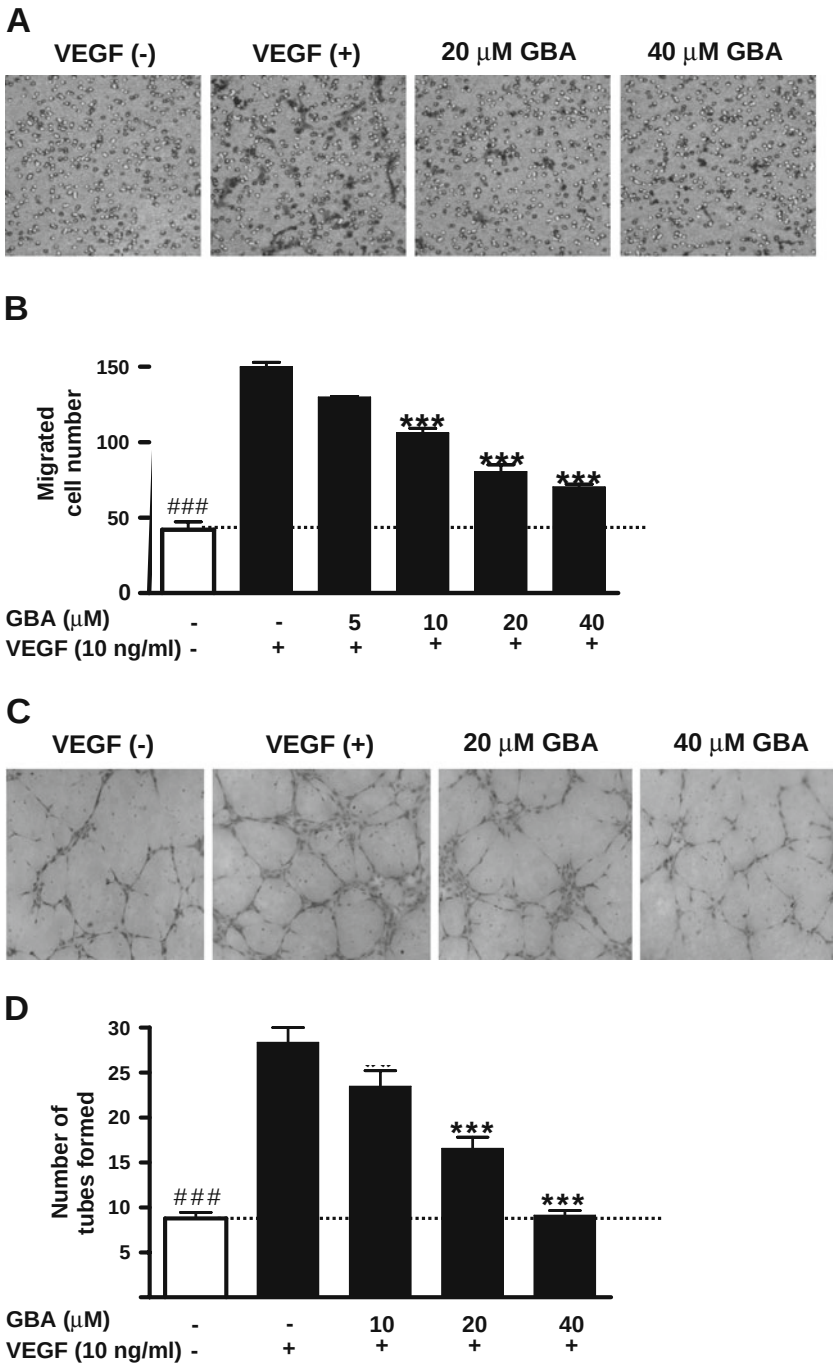

Fig. 3 Effects of GBA on VEGF-induced HUVEC motility/invasion (**A** & **B**) and capillary differentiation (**C** & **D**). **A** VEGF-induced chemotactic migration/invasion. HUVECs were mixed with indicated concentration of GBA, placed in the upper chamber of 48-well chemotactic chamber on top of a gelatin-coated membrane. Representative photomicrographs of migrated cells to the under side (stained dark) are shown. **B** Quantification of the migrated cells. **C** VEGF-induced tube formation of HUVECs on Matrigel. Cells were treated with indicated concentration of GBA and then plated on growth factor-reduced Matrigel in the absence or presence of VEGF (10 ng/ml) for 18 h. Representative fields of "capillary tubes" formed are shown. **D** Quantification of the tubes formed per 100× field. All data are presented as means ± SE; $n = 3$. $^{###}p < 0.001$ compared with VEGF-untreated control, $^{***}p < 0.001$ compared with VEGF-treated control.

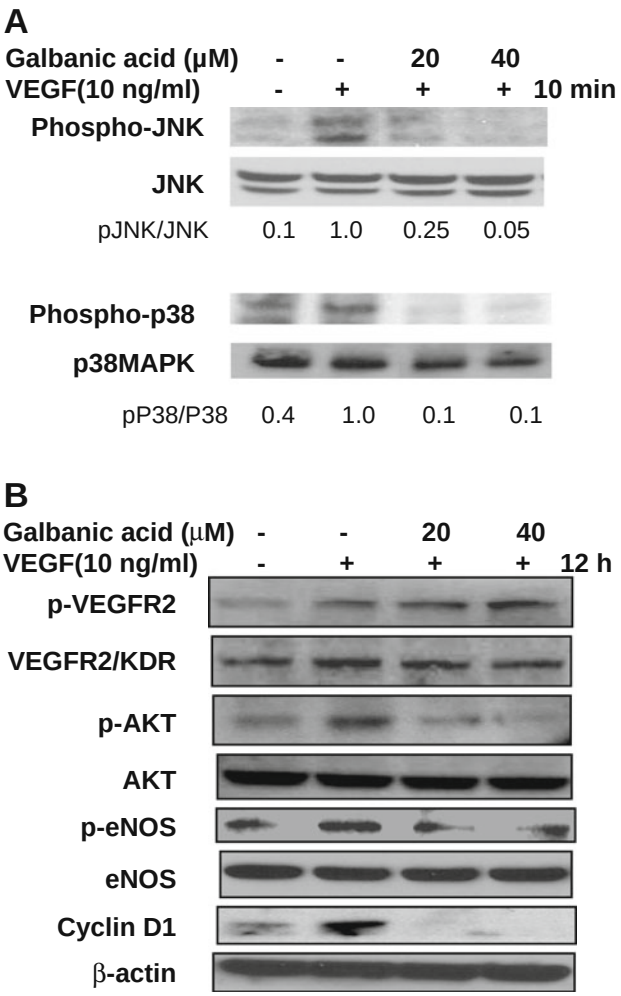

Fig. 4 Galbanic acid inhibits VEGF-induced protein kinases, and other endothelial molecular targets. **A** Effect of GBA on the phosphorylation of JNK and p38MPAK families in VEGF-treated HUVECs. HUVECs were pretreated with various concentrations of GBA for 30 min and stimulated with VEGF 10 ng/ml for 10 min. **B** Effect of GBA on the phosphorylation of VEGF-R2 (KDR), AKT, eNOS and expression of cyclin D1 in VEGF-treated HUVECs. HUVECs were pretreated with various concentrations of GBA for 30 min and stimulated with VEGF 10 ng/ml for 12 h.

GBA, with a greater sensitivity for HUVEC than for LLC cells.

Effect of GBA on VEGF-Induced Migration/Invasion of HUVECs

Since endothelial motility and matrix degradation and remodeling are crucial to the angiogenesis response, we evaluated the effect of GBA on endothelial cell migration/invasion using a modified Borden chamber assay (Fig. 3a). Galbanic acid significantly suppressed VEGF-stimulated migration through a gelatin-coated membrane in a concentration-dependent manner with IC_{50} ~ 20 μM, in reference to basal motility (Fig. 3b).

Effect of GBA on VEGF-Induced Tube Formation of HUVECs

VEGF stimulates the angiogenic differentiation of HUVECs (capillary-like tube formation) on Matrigel (Fig. 3c). The number of tube-like structures induced by VEGF was 28±1.7 *vs.* 8±0.7 for basal level (per field). GBA disrupted the tube formation to 17±1.2 and 9±0.5 tubes at 20 and 40 μM, respectively (Fig. 3d). The concentration of GBA to achieve a 50% inhibition of VEGF-induced tube formation above the basal level was ~15 μM.

Effect of GBA on Signaling Activities of Protein Kinases and VEGF Targets in VEGF-Treated HUVECs

VEGF binds its receptors, VEGFR1 and VEGFR2. VEGFR2 (KDR/Flk) has stronger tyrosine kinase activity, transducing the major signals for vascular endothelial responses in angiogenesis (10,19), including activating PI3K-AKT for survival and proliferation, stimulating motility and actin reorganization through Rac as well as through p38MAPK, and activation of ERK, c-Jun N-terminal kinase (JNK) for DNA synthesis and endothelial nitric oxide synthase (eNOS) for vascular permeability. To determine whether the observed anti-angiogenic attributes of GBA were associated with an attenuation of VEGFR2 auto-phosphorylation or its downstream targets, Western blot analysis was performed on whole cell lysate from HUVECs pre-treated with GBA and then stimulated by VEGF for 10 min for JNK and p38MAPK and 12 h for AKT, eNOS and cyclin D expression. Galbanic acid decreased the phosphorylation of JNK and p38MAPK in VEGF-treated HUVECs to basal level (Fig. 4a). GBA decreased the VEGF-induced phosphorylation of AKT and eNOS (Fig. 4b) and blocked VEGF-induced cyclin D1 expression (Fig. 4b) at 20 and 40 μM in cells treated with VEGF for 12 h without inhibiting VEGF-induced VEGFR-2 auto-phosphorylation or VEGFR-2 protein abundance (Fig. 4b). Together, the data suggested that non-cytotoxic concentrations of GBA inhibited VEGF-induced signaling thorough key kinases and proteins in HUVECs downstream of VEGFR2.

Effect of GBA on Functional Angiogenesis in Matrigel Plug Assay

Since the *in vitro* test results above suggest potential anti-angiogenic activity of GBA *in vivo*, we next examined the impact of inclusion of GBA in Matrigel plugs on VEGF-induced microvessel formation (Fig. 5a). The extent of functional angiogenesis was indirectly evaluated by measuring the contents of hemoglobin (Hb) in Matrigel plug isolated from mice. Galbanic acid significantly reduced the

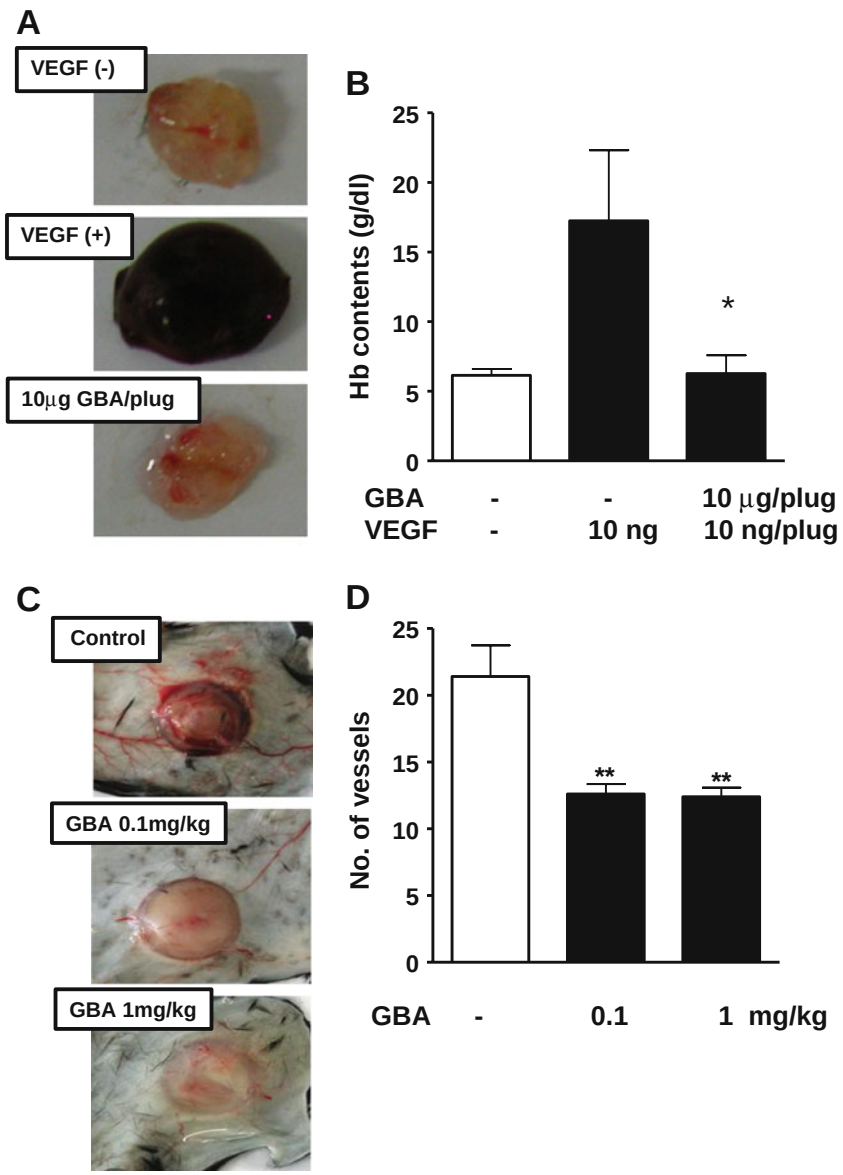

Fig. 5 Effect of GBA on functional angiogenesis *in vivo*. **A** Matrigel plug model. GBA (20 μg/ml or ~10 μg/plug), VEGF (20 ng/ml, ~10 ng/plug) and heparin (10 U/ml) were mixed with growth factor-reduced Matrigel, and 0.5 ml of the mixture was injected s.c. into C57BL/6 mice. After 7 days, mice were sacrificed, and the Matrigel plug was removed. The pictures show typical appearance of Matrigel plugs excised from mice from different groups. **B** The level of hemoglobin (Hb) was measured from ground Matrigel plugs. Each value represents as mean ± SE; $n = 5$. $^{*}p < 0.05$ compared with VEGF-control. **C** Effect of GBA on cancer-induced angiogenesis. Mice were intra-dermally inoculated with LLC cells and received *i.p.* injection of GBA (0.1 mg/kg/day or 1 mg/kg/day). Tumor inoculated sites were dissected from vehicle- or GBA-treated mice (Day 3–9 after the tumor inoculation). The pictures show the appearance of typical inoculation sites. **D** Tumor-supplying vessels were counted. Data were presented as mean ± SE; $n = 7$. $^{**}p < 0.01$ compared with PBS-treated control.

level of Hb level from 17.2±5.1 g/dl in VEGF-treated control to 6.3±1.3 g/dl at an inclusion rate of 20 μg GBA/ml Matrigel (~10 ng/plug), essentially attenuated back to the basal level (Fig. 5b).

Effect of GBA on Tumor Cell-Induced Angiogenesis

To confirm inhibitory activity of GBA against angiogenesis induced *in vivo* by tumor cells, LLC cells were inoculated intradermally onto the back skin of mice, and GBA was administered intraperitoneally at doses of 0.1 and 1 mg/kg/day for 7 days (Days 3–9 after tumor inoculation) (Fig. 5c). Galbanic acid reduced the number of vessels oriented to the tumor cell mass by over 40% (Fig. 5d), indicating an inhibition of tumor-induced angiogenesis. No acute side effects, such as hair loss, lethargy and mortality, were detected.

Effect of GBA on the Growth of LLC in Mice

To examine whether the anti-angiogenic actions of GBA translated to anti-tumor activity *in vivo*, we treated C57BL/6 mice subcutaneously implanted with the highly angiogenesis-dependent LLC allografts with an *i.p.* injection of GBA every day from Day 12 after tumor inoculation (~50 mm^3). Tumors grew rapidly and reached an average volume of 720 mm^3 on Day 18 after the inoculation of LLC cells, whereas tumor volume and weight were significantly inhibited by treatment of GBA at a dose of 1 mg/kg from Day 12 to Day 18, compared with vehicle-treated control

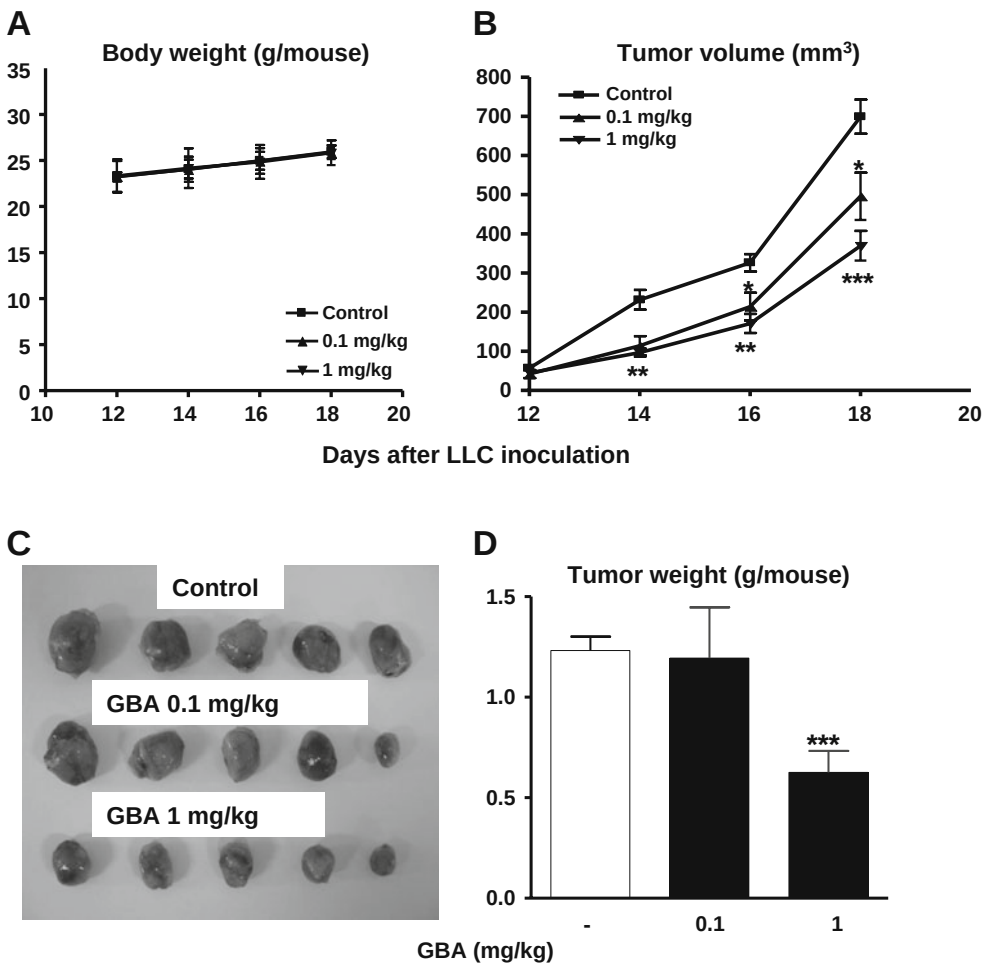

Fig. 6 Galbanic acid inhibits LLC allograft growth *in vivo*. LLC cells were injected s.c. (5×10^5 in 200 μl PBS) into the right flank of C57BL/6 mice. After the tumor had established (12 days; ~ 50 mm^3), the mice were given *i.p.* injection of GBA (0.1 mg/kg/day or 1 mg/kg/day). **A** The mouse body weight. **B** Tumor volume measured with a caliper. **C** Dissected tumors after necropsy. **D** Tumor weight after necropsy. Data were presented as mean ± SE; $n = 5$. *$p < 0.05$, **$p < 0.01$ and ***$p < 0.001$ compared with control.

group (Fig. 6b–d). No acute side effects, such as body weight loss (Fig. 6a), hair loss, lethargy and mortality, were detected.

Effects of GBA on CD34 and Ki-67 Expression in LLC Tumor Section

To verify that anti-angiogenesis was involved in the LLC growth inhibition *in vivo* by GBA, we stained tumor sections with an antibody to the endothelial cell surface protein CD34, which marks newly formed microvessels (Fig. 7a, 100 × magnification). The CD34 (+) microvessels were decreased by more than 58% in the GBA-treated mice at the 1 mg/kg dose (Fig 7a and c). In addition, the *in vivo* LLC growth-inhibitory efficacy of GBA was also associated with decreased proliferative biomarker protein Ki-67 nuclear staining in the LLC cells (Fig. 7b and d, 400 × magnification).

DISCUSSION

In addition to being a food spice, *Ferula assafoetida* L. has been traditionally used as a sedative, carminative, antispasmodic and diuretic agent (28). Moreover, *Ferula assafoetida* L. has been reported to have various biological effects such as antibacterial (29), anti-carcinogenic (30,31), anti-thrombotic (32), anti-oxidant (30), anti-inflammatory (33) and anti-hepatotoxic activities (34). The anti-tumor mechanisms have not been well studied. Given the role of angiogenesis in tumor growth and progression (1,2), the present study was designed to examine the anti-angiogenic activities of GBA, a coumarin-containing compound (Fig. 1a), as a contributing mechanism. This was in part inspired by our finding of a strong anti-angiogenic efficacy of the coumarin-containing compound farnesiferol C isolated from the same *Ferula assafoetida* resin (12). Angiogenesis is an attractive target for novel anti-cancer therapies or cancer chemoprevention because of the many advantages that it may offer, including better agent accessibility to endothelial cells than to tumor cells, independence of tumor cell drug resistance mechanisms and broad applicability to many tumor types (8).

Our data have demonstrated that GBA was seemingly more cytocidal to HUVEC (Fig. 1b) than to the LLC cells (Fig. 2a). The non-cytotoxic concentrations of GBA were

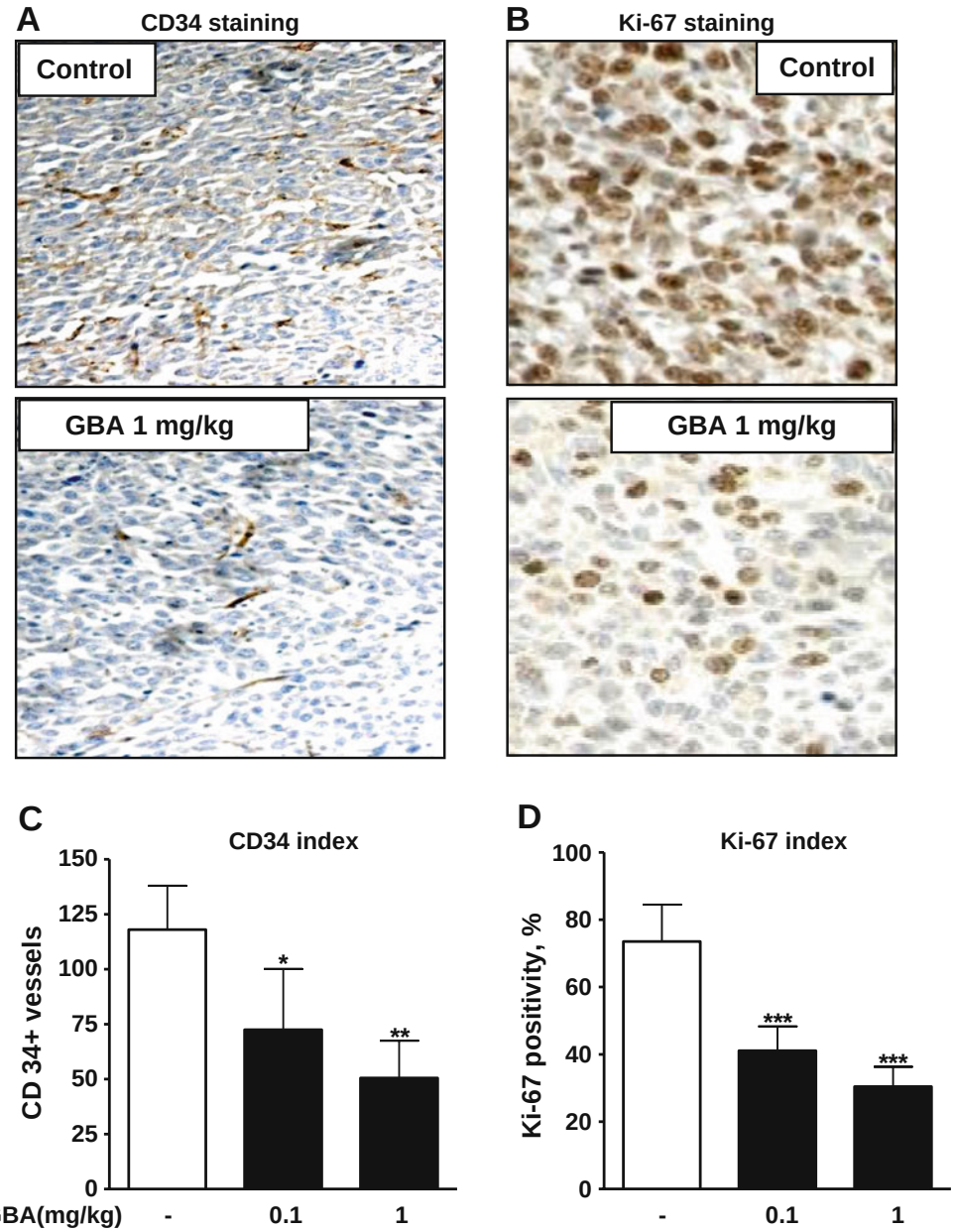

Fig. 7 Angiogenesis and proliferative indices of GBA-treated LLC tumors. **A** Representative immuno-histochemical staining (dark brown, endothelial cell surface) for CD34 in tumor sections (100×). **B** Representative immuno-histochemical staining (dark brown, nuclear) for Ki-67 in tumor sections (400×). **C** CD34 index determined by number of positive vessels per field. **D** Ki-67 index determined as% positive nuclei. Data were presented as mean ± SE; $n = 5$. *$p < 0.05$, **$p < 0.01$ and ***$p < 0.001$ compared with control.

also more anti-proliferative for the HUVEC (Fig. 1c) than for LLC (Fig. 2b) and suppressed VEGF-stimulated proliferation (Fig. 1c) and migration/invasion of HUVECs (Fig. 3a&b) and inhibited angiogenic differentiation of HUVECs on Matrigel (Fig. 3c&d) in concentration-dependent manners. In terms of molecular targeting mechanisms, our preliminary exploration showed that GBA inhibited a number of protein kinases downstream of VEGFR2 in the VEGF-stimulated HUVEC model (Fig. 4), including AKT (survival and proliferation) and JNK (proliferation), p38MAPK (motility) and the expression of eNOS (permeability) and cyclin D1 (activator of CDK4/6 to promote G_o/G_1 progression). Specific activation of each of these signaling cassettes has been shown to be dependent on the type of extra-cellular stimuli. The PTEN/AKT and ERK pathways are activated by growth factors and angiogenic cytokines (e.g., VEGF), while the JNK, p38 pathways are activated by environmental stress in addition to growth factor signaling (35). Activation of these pathways in endothelial cells is a critical step in the angiogenic response cascades, as individual MAPK branches have been shown to separately drive endothelial cell proliferation, migration, invasion and differentiation during angiogenesis (36,37). Our observed rapid decrease (within 10 min) by GBA of the pJNK1/2 and p38MAPK and subsequent decrease of pAKT and eNOS (permeability) and cyclin D1 (G1 progression) (detected at 12 h) without affecting VEGFR2 auto-phosphorylation in VEGF-

stimulated HUVEC (Fig. 4) suggest these downstream components might be targeted by GBA for the anti-angiogenic cellular responses.

In vitro anti-angiogenic effects of GBA were confirmed in *in vivo* models. Galbanic acid significantly reduced the level of Hb in VEGF-treated Matrigel at an inclusion rate of 10 μg/plug or 20 μg/ml (Fig. 5a–b). In addition, the anti-angiogenic effect of GBA against LLC cell-induced angiogenesis was confirmed in an intradermal model (Fig. 5c–d). Furthermore, its *in vivo* inhibitory efficacy against the growth of LLC allograft (Fig. 6b–d) correlated with decreased microvessel density (Fig. 7a and c). It is noteworthy that the potency of the effective dose of 1 mg GBA per kg body weight against LLC allograft growth is very impressive and would be on par with or even better than the taxane drugs for *in vivo* anti-cancer activity in the LLC model (38). Future work will need to address the pharmacokinetics of GBA and its cancer cell uptake as well as their metabolism to shed light on whether GBA or key metabolite(s) mediates the anti-angiogenic and anti-cancer activities *in vivo*.

In addition to the decreased expression of CD34 angiogenic index in the GBA-treated tumor sections (Fig. 7a and c), we have observed decreased Ki-67 labeling of the nuclei of the GBA-treated LLC tumors (Fig. 7b and d). Our examination of the direct exposure effect of GBA on LLC cells revealed anti-proliferative action without apoptosis (Fig. 2), albeit less potent than against the HUVEC (Fig. 1). Consistent with the rather non-cytocidal effect in LLC cells, our studies with prostate cancer (PCa) cell lines (LNCaP, PC-3, DU-145) (Zhang, *et al.*, submitted elsewhere) have shown a lack of acute apoptotic effect at 80 μM or lower. However, we observed a down-regulation of androgen receptor (AR) and its signaling and G_1 arrest effects through inhibiting cyclin D1 expression and CDK/RB/E2F pathway in AR-expressing PCa cells in the similar concentration ranges of GBA (10–40 μM) that inhibit vascular endothelial responses *in vitro*.

In summary, GBA exposure inhibited VEGF-induced proliferation, migration/invasion and capillary differentiation (tube formation) in HUVECs, and VEGF-induced angiogenesis in Matrigel plug assay. Galbanic acid treatment by i.p. delivery suppressed the LLC-induced angiogenesis and the *in vivo* growth of LLC allografts, in association with reduced CD34 microvessel density index and Ki-67 proliferative index. Taken together, these findings suggest that GBA may be a cancer chemopreventive drug candidate, at least in part, via its anti-angiogenic activity and an inhibition of key endothelial kinase pathways and in part via an anti-proliferative effect on cancer cell growth. Additional studies are warranted to confirm the anti-cancer efficacy of GBA and elucidate its pharmacokinetics, cellular uptake and metabolism.

ACKNOWLEDGMENTS

This work was supported by Medical Research Center (MRC) grant (No. 2009-0063466) (S.H. Kim) and Hormel Foundation and NIH grant CA136953 (J. Lu). All authors declare no personal or financial conflict of interests.

REFERENCES

1. Folkman J. Angiogenesis in cancer, vascular, rheumatoid and other disease. Nat Med. 1995;1(1):27–31.
2. Hanahan D, Folkman J. Patterns and emerging mechanisms of the angiogenic switch during tumorigenesis. Cell. 1996;86(3):353–64.
3. Carmeliet P, Jain RK. Angiogenesis in cancer and other diseases. Nature. 2000;407(6801):249–57.
4. Folkman J. Fundamental concepts of the angiogenic process. Curr Mol Med. 2003;3(7):643–51.
5. Krupinski J, Stroemer P, Slevin M, Marti E, Kumar P, Rubio F. Three-dimensional structure and survival of newly formed blood vessels after focal cerebral ischemia. NeuroReport. 2003;14(8):1171–6.
6. Slevin M, Krupinski J, Kumar P, Gaffney J, Kumar S. Gene activation and protein expression following ischaemic stroke: strategies towards neuroprotection. J Cell Mol Med. 2005;9(1):85–102.
7. Slevin M, Kumar P, Gaffney J, Kumar S, Krupinski J. Can angiogenesis be exploited to improve stroke outcome? Mechanisms and therapeutic potential. Clin Sci (Lond). 2006;111(3):171–83.
8. Tosetti F, Ferrari N, De Flora S, Albini A. Angioprevention': angiogenesis is a common and key target for cancer chemopreventive agents. FASEB J. 2002;16(1):2–14.
9. El Sayed KA. Natural products as angiogenesis modulators. Mini Rev Med Chem. 2005;5(11):971–93.
10. Ellis LM, Hicklin DJ. VEGF-targeted therapy: mechanisms of anti-tumour activity. Nat Rev Cancer. 2008;8(8):579–91.
11. Abd El-Razek MH, Ohta S, Ahmed AA, Hirata T. Sesquiterpene coumarins from the roots of Ferula assa-foetida. Phytochemistry. 2001;58(8):1289–95.
12. Lee JH, Choi S, Lee Y, *et al.* Herbal compound farnesiferol C exerts antiangiogenic and antitumor activity and targets multiple aspects of VEGFR1 (Flt1) or VEGFR2 (Flk1) signaling cascades. Mol Cancer Ther. 2010;9(2):389–99.
13. Lee SG, Ryu SY, Ahn JW. Reinvestigation of the structure of galbanic acid by 2D NMR techniques including 2D inadequate. Bull Korean Chem Soc. 1998;19(3):384–6.
14. Mansurov MM, Martirosov MS. Effect of the sodium salt of galbanic acid on thrombocyte aggregation. Farmakol Toksikol. 1988;51(1):47–8.
15. Bobek V, Kovarik J. Antitumor and antimetastatic effect of warfarin and heparins. Biomed Pharmacother. 2004;58(4):213–9.
16. Nakashima T, Hirano S, Agata N, *et al.* Inhibition of angiogenesis by a new isocoumarin, NM-3. J Antibiot (Tokyo). 1999;52(4):426–8.
17. Nam NH, Kim Y, You YJ, Hong DH, Kim HM, Ahn BZ. New constituents from Crinum latifolium with inhibitory effects against tube-like formation of human umbilical venous endothelial cells. Nat Prod Res. 2004;18(6):485–91.
18. Carmeliet P. VEGF as a key mediator of angiogenesis in cancer. Oncology. 2005;69 Suppl 3:4–10.
19. Kowanetz M, Ferrara N. Vascular endothelial growth factor signaling pathways: therapeutic perspective. Clin Cancer Res. 2006;12(17):5018–22.

20. Jaffe EA, Nachman RL, Becker CG, Minick CR. Culture of human endothelial cells derived from umbilical veins. Identification by morphologic and immunologic criteria. J Clin Invest. 1973;52(11):2745–56.
21. Huh JE, Lee EO, Kim MS, *et al.* Penta-O-galloyl-beta-D-glucose suppresses tumor growth via inhibition of angiogenesis and stimulation of apoptosis: roles of cyclooxygenase-2 and mitogen-activated protein kinase pathways. Carcinogenesis. 2005;26(8):1436–45.
22. Jost LM, Kirkwood JM, Whiteside TL. Improved short- and long-term XTT-based colorimetric cellular cytotoxicity assay for melanoma and other tumor cells. J Immunol Methods. 1992;147(2):153–65.
23. Grant DS, Kinsella JL, Fridman R, *et al.* Interaction of endothelial cells with a laminin A chain peptide (SIKVAV) in vitro and induction of angiogenic behavior *in vivo*. J Cell Physiol. 1992;153(3):614–25.
24. Lee HJ, Lee EO, Rhee YH, *et al.* An oriental herbal cocktail, ka-mi-kae-kyuk-tang, exerts anti-cancer activities by targeting angiogenesis, apoptosis and metastasis. Carcinogenesis. 2006;27(12):2455–63.
25. Passaniti A, Taylor RM, Pili R, *et al.* A simple, quantitative method for assessing angiogenesis and antiangiogenic agents using reconstituted basement membrane, heparin, and fibroblast growth factor. Laboratory investigation; a journal of technical methods and pathology. 1992;67(4):519–28.
26. Alessandri G, Filippeschi S, Sinibaldi P, *et al.* Influence of gangliosides on primary and metastatic neoplastic growth in human and murine cells. Cancer Res. 1987;47(16):4243–7.
27. Giavazzi R, Campbell DE, Jessup JM, Cleary K, Fidler IJ. Metastatic behavior of tumor cells isolated from primary and metastatic human colorectal carcinomas implanted into different sites in nude mice. Cancer Res. 1986;46(4 Pt 2):1928–33.
28. Eigner D, Scholz D. Ferula asa-foetida and Curcuma longa in traditional medical treatment and diet in Nepal. J Ethnopharmacol. 1999;67(1):1–6.
29. Garg DK, Banerjea AC, Verna J. The role of intestinal Clostidia and the effect of asafetida (Hing) and alcohol in flatulence. Indian J Microbiol. 1980;20(3):194–7.
30. Mallikarjuna GU, Dhanalakshmi S, Raisuddin S, Rao AR. Chemomodulatory influence of Ferula asafoetida on mammary epithelial differentiation, hepatic drug metabolizing enzymes, antioxidant profiles and N-methyl-N-nitrosourea-induced mammary carcinogenesis in rats. Breast Cancer Res Treat. 2003;81(1):1–10.
31. Unnikrishnan MC, Kuttan R. Tumour reducing and anticarcinogenic activity of selected spices. Cancer Lett. 1990;51(1):85–9.
32. Mansurov MM. Effect of Ferula asafetida on the blood coagulability. Med Zh Uzb. 1967;1967(6):46–9.
33. Rahlfs VW, Mossinger P. Asa foetida in the treatment of the irritable colon: a double-blind trial (author's transl). Dtsch Med Wochenschr. 1979;104(4):140–3.
34. Soni KB, Rajan A, Kuttan R. Inhibition of aflatoxin-induced liver damage in ducklings by food additives. Mycotoxin Res. 1993;9(1):22–7.
35. Roberts PJ, Der CJ. Targeting the Raf-MEK-ERK mitogen-activated protein kinase cascade for the treatment of cancer. Oncogene. 2007;26(22):3291–310.
36. Depeille PE, Ding Y, Bromberg-White JL, Duesbery NS. MKK signaling and vascularization. Oncogene. 2007;26(9):1290–6.
37. Murphy DA, Makonnen S, Lassoued W, Feldman MD, Carter C, Lee WM. Inhibition of tumor endothelial ERK activation, angiogenesis, and tumor growth by sorafenib (BAY43-9006). Am J Pathol. 2006;169(5):1875–85.
38. Bissery MC, Guenard D, Gueritte-Voegelein F, Lavelle F. Experimental antitumor activity of taxotere (RP 56976, NSC 628503), a taxol analogue. Cancer Res. 1991;51(18):4845–52.